Journal of Physiology (2002), **542.3**, *pp.* 699–710
DOI: 10.1113/jphysiol.2002.020677

www.jphysiol.org

The $Ca_V2.3$ Ca^{2+} channel subunit contributes to R-type Ca^{2+} currents in murine hippocampal and neocortical neurones

Dmitry Sochivko *, Alexey Pereverzev †, Neil Smyth ‡, Cornelia Gissel †, Toni Schneider † and Heinz Beck *

* *Department of Epileptology, University of Bonn Medical Center, Sigmund-Freud Str. 25, 53105 Bonn, Germany,* † *Department of Neurophysiology, University of Cologne, Robert-Koch Str. 39, 50931 Cologne, Germany and* ‡ *Department of Biochemistry, University of Cologne, Joseph-Stelzmann Str. 52, 50931 Cologne, Germany*

Different subtypes of voltage-dependent Ca^{2+} currents in native neurones are essential in coupling action potential firing to Ca^{2+} influx. For most of these currents, the underlying Ca^{2+} channel subunits have been identified on the basis of pharmacological and biophysical similarities. In contrast, the molecular basis of R-type Ca^{2+} currents remains controversial. We have therefore examined the contribution of the $Ca_V2.3$ (α_{1E}) subunits to R-type currents in different types of central neurones using wild-type mice and mice in which the $Ca_V2.3$ subunit gene was deleted. In hippocampal CA1 pyramidal cells and dentate granule neurones, as well as neocortical neurones of wild-type mice, Ca^{2+} current components resistant to the combined application of ω-conotoxin GVIA and MVIIC, ω-agatoxin IVa and nifedipine ($I_{Ca,R}$) were detected that were composed of a large R-type and a smaller T-type component. In $Ca_V2.3$-deficient mice, $I_{Ca,R}$ was considerably reduced in CA1 neurones (79 %) and cortical neurones (87 %), with less reduction occurring in dentate granule neurones (47 %). Analysis of tail currents revealed that the reduction of $I_{Ca,R}$ is due to a selective reduction of the rapidly deactivating R-type current component in CA1 and cortical neurones. In all cell types, $I_{Ca,R}$ was highly sensitive to Ni^{2+} (100 μM: 71–86 % block). A selective antagonist of cloned $Ca_V2.3$ channels, the spider toxin SNX-482, partially inhibited $I_{Ca,R}$ at concentrations up to 300 nM in dentate granule cells and cortical neurones (50 and 57 % block, EC_{50} 30 and 47 nM, respectively). $I_{Ca,R}$ in CA1 neurones was significantly less sensitive to SNX-482 (27 % block, 300 nM SNX-482). Taken together, our results show clearly that $Ca_V2.3$ subunits underlie a significant fraction of $I_{Ca,R}$ in different types of central neurones. They also indicate that $Ca_V2.3$ subunits may give rise to Ca^{2+} currents with differing pharmacological properties in native neurones.

(Resubmitted 17 March 2002; accepted after revision 15 May 2002)
Corresponding author H. Beck: Department of Epileptology, University of Bonn Medical Center, Sigmund-Freud Str. 25, D-53105 Bonn, Germany. Email: heinz.beck@ukb.uni-bonn.de

Voltage-dependent Ca^{2+} channels are one of the main Ca^{2+} entry pathways into neuronal cells and are of central importance in coupling action potential firing to Ca^{2+} influx. Therefore, considerable interest has focused on the molecular structures underlying different types of Ca^{2+} currents in neurones. Most native neurones display several types of high-threshold Ca^{2+} currents, which can be pharmacologically classified as L-, N-, P/Q- and R-type (Ertel *et al.* 2000). In addition, most neurones express T-type Ca^{2+} channels with a low threshold of activation, a pronounced time-dependent inactivation and a slow deactivation (Cribbs *et al.* 1998; Lambert *et al.* 1998; Lee *et al.* 1999*a*). It is generally accepted that all of these Ca^{2+} channels are formed by one of a number of pore-forming α_1 subunits $\alpha_{1A\text{-}I}$ and α_{1S} (Birnbaumer *et al.* 1994; Ertel *et al.* 2000), in addition to ancillary subunits (Hofmann *et al.* 1999). On the basis of pharmacological and biophysical similarities, α_{1A}, α_{1B} and $\alpha_{1C/D}$ subunits are thought to underlie P/Q-, N- and L-type Ca^{2+} currents in native neurones, respectively (Hofmann *et al.* 1999), while the $\alpha_{1G\text{-}I}$ subunits give rise to T-type Ca^{2+} currents (Perez-Reyes, 1999).

In contrast, the molecular basis of R-type currents in different types of native neurones is less clear. The R-type current was first described as a component that is resistant to the combined application of organic Ca^{2+} channel antagonists ($I_{Ca,R}$; Zhang *et al.* 1993; Randall & Tsien, 1995). Subsequently, R-type currents with diverse biophysical properties were described in different types of CNS neurones (Eliot & Johnston, 1994; Foehring *et al.* 2000; Magistretti *et al.* 2000; Scamps *et al.* 2000; Tottene *et al.* 2000). The prime candidate as a pore-forming subunit of R-type currents is the $Ca_V2.3$ (α_{1E}) subunit. However, the identification of current components carried by the $Ca_V2.3$ subunit in different subtypes of native neurones has been

D. Sochivko and A. Pereverzev contributed equally to this work.

hampered by the limited number of specific blockers targeting this subunit (Randall & Tsien, 1995). Indeed, the only selective blocker of $Ca_V2.3$ in expression systems, the spider toxin SNX-482, fails to block R-type currents in many native cells (Newcomb *et al.* 1998). Therefore, transgenic and antisense inhibition experiments have been employed to address the contribution of $Ca_V2.3$ to R-type currents in native neurones, with controversial results. The antisense inhibition of $Ca_V2.3$ subunit expression suggests that this subunit underlies the major portion of R-type currents in cultured cerebellar granule neurones (Tottene *et al.* 2000). However, functional analysis of cerebellar granule cell and dorsal root ganglion cell cultures prepared from mice in which the $Ca_V2.3$ gene has been deleted showed that only a minor portion of the R-type current results from expression of $Ca_V2.3$ (Wilson *et al.* 2000), whereas $Ca_V2.3$ subunits give rise to a large fraction of the R-type current in amygdala neurones (Lee *et al.* 2002). Similar divergent results have been obtained for the pharmacological properties of the putative $Ca_V2.3$-mediated current in these preparations (Tottene *et al.* 2000; Wilson *et al.* 2000).

In view of the controversy regarding the molecular identity of the R-type current, we have addressed this question in different CNS cell types using mice in which the $Ca_V2.3$ subunit has been deleted. We demonstrate that $Ca_V2.3$ subunits underlie a significant portion of the R-type current in hippocampal CA1 and dentate granule neurones, as well as in cortical neurones.

METHODS

Gene targeting of $Ca_V2.3$ (α_{1E}) by homologous recombination

All animal experiments were carried out according to the guidelines provided by the University of Cologne and the University of Bonn animal welfare committee. For the generation of the targeting construct, genomic clones containing exons 2 and 3 of the *cacna1E* gene of 129/Sv mice were obtained from a genomic library (lambda fix-II, Stratagene). A 14 kb genomic fragment was subcloned into *Sal*I digested pBluescript-SK vector and the *Hin*dIII–*Sal*I fragment containing exons 2 and 3 was completely sequenced. The loxP-flanked neomycin cassette was inserted into the *Nsi*I site between exons 2 and 3. The third loxP site was introduced downstream of the *Hin*dIII site by a PCR-based strategy amplifying a 421-bp-long DNA fragment between the *Hin*dIII site and the *Pfl*mI site. The proper amplification was confirmed by sequencing of the DNA fragment. The recombinant *Hin*dIII–*Pfl*mI fragment containing the third loxP site was then introduced into the targeting vector.

The gene locus of $Ca_V2.3$ was targeted by homologous recombination in E14.1 embryonic stem (ES) cells. Correctly targeted clones, as shown by Southern blot analysis, were transiently transfected with the pCre-pac vector. The efficiency of the expression of the *Cre*-recombinase was improved by imposing a 2 day treatment with puromycin as a selection marker (Taniguchi *et al.* 1998). Surviving clones were analysed for the loss of the Neo cassette and the presence of a loxP-flanked exon 2 (= fl). ES cell subclone Tα1E1E8PuNr6 had such a type-II deletion and was injected into C57Bl/6 blastocysts. Resulting male chimeras were bred to C57Bl/6 females and the $Ca_V2.3$(fl/+) genotype of agouti-coloured offspring was determined by Southern blot analysis.

Disruption of *cacna1E in vivo* using *Cre*-deleter mice

The *cacna1E* gene was disrupted by deleting a region containing exon 2 *in vivo* on mating $Ca_V2.3$(fl/+) mice with deleter mice (Schwenk *et al.* 1995), which express *Cre*-recombinase constitutively under the control of a cytomegalovirus (CMV) promoter. After mating of $Ca_V2.3$(fl/+) and deleter mice, the offspring were genotyped by Southern blot analysis. In 20 out of 83 pups (24 %) exon 2 was deleted by *Cre*-mediated recombination. Heterozygous $Ca_V2.3$(+/−) mice were intercrossed to derive $Ca_V2.3$-deficient mice. Genotyping the offspring of such matings showed a Mendelian inheritance with 27 of 106 (29 %) of newborn pups being $Ca_V2.3$(−/−) mice, which leads to the conclusion that a general ablation of $Ca_V2.3$ is not embryonically lethal. The $Ca_V2.3$(−/−) mice displayed normal sexual activity and reproduction, and they exhibited no obvious anatomical abnormalities. Age-matched C57Bl/6 mice were used as control animals throughout the following experiments. Mice were housed under conditions of constant temperature (22–23 °C), with light from 7.00 a.m. to 7.00 p.m., and access to food and water *ad libitum*.

Isolation of microsomal membranes and immunoblotting

Brain microsomes were isolated according to standard procedures (Flockerzi *et al.* 1986), as described in detail by Pereverzev *et al.* (1998). Half of a brain was used to isolate microsomes without freezing the tissue. Aliquots of microsomal membranes were stored at −80 °C.

Preparation of acutely isolated cells

Isolated hippocampal or neocortical neurones were prepared as described previously (Beck *et al.* 1998). Experiments on $Ca_V2.3$(−/−) and (+/+) mice were interleaved. Mice were aged 2–15 months. For comparisons of $Ca_V2.3$(−/−) and (+/+) animals, mice were always age-matched. Animals were decapitated under deep ether anaesthesia and the brain rapidly removed and placed in ice-cold artificial cerebrospinal fluid (ACSF) containing (mM): NaCl 125, KCl 3, $CaCl_2$ 2, $MgCl_2$ 1, NaH_2PO_4 1.25, glucose 20 and $NaHCO_3$ 25 (pH 7.4, osmolarity 305 mosmol l^{-1}, 95 % CO_2–5 % O_2). Hippocampal or neocortical slices (400 μm) were prepared with a vibratome and transferred to a storage chamber with ACSF where they were maintained at room temparature. After an equilibration period of at least 60 min, enzymatic digestion was carried out for 10 min at 37 °C and 5 min at room temperature in 5 ml of incubation medium containing (mM): sodium methanesulfonate 145, KCl 3, $CaCl_2$ 0.5, $MgCl_2$ 1, Hepes 10, glucose 15 and pronase (protease type XIV, Sigma) 2 mg ml^{-1} (pH 7.4, osmolarity 310 mosmol l^{-1}, 100 % O_2). After washing with enzyme-free incubation medium, the area of interest (CA1 region, dentate gyrus or neocortex) was dissected and triturated with fire-polished glass pipettes, and the cell suspension placed in a Petri dish. The isolated cells were superfused with an extracellular solution containing (mM): sodium methanesulfonate 125, TEA-Cl 20, 4-aminopyridine (4-AP) 4, $BaCl_2$ 5, $MgCl_2$ 1, KCl 3, glucose 10, Hepes 10, TTX 0.5 μM (pH 7.4, osmolarity 315 mosmol l^{-1}). In the CA1 and the cortical preparation, dissociated neurones that displayed a pyramidal shape, a single well-defined apical dendrite and smaller basal dendrites were selected for recording. In the dentate gyrus, smaller neurones with an ovoid soma and a single apical dendrite were selected. The $Ca_V2.3$-selective antagonist SNX-482 was obtained from the Peptide Institute (Osaka, Japan).

Other Ca^{2+} channel toxins were obtained from Bachem Biochemica (Heidelberg, Germany). All other chemicals were obtained from Sigma. Stock solutions of these toxins (0.2–1 mM) were prepared in deoxygenated solutions containing 0.1 % bovine serum albumin (BSA), 100 mM NaCl, 10 mM Trizma, 1 mM EDTA, pH 7.5 (HCl). Toxins were applied in extracellular solution containing 0.1 mg ml^{-1} cytochrome *c* to prevent unspecific binding to tubing. Nifedipine stock solutions were prepared in DMSO (10 mM). The different extracellular solutions were applied with a superfusion pipette placed at a distance of 30–50 μm from the cell body. The superfusion rate was adjusted by hydrostatic pressure.

Patch-clamp whole-cell recording

Patch pipettes with a resistance of 3–4 MΩ were fabricated from borosilicate glass capillaries and filled with an intracellular solution containing (mM): caesium methanesulfonate 87.5, TEA-Cl 20, $CaCl_2$ 0.5, $MgCl_2$ 5, BAPTA 5, Hepes 10, glucose 10, adenosine-5′-triphosphate (Na_2-ATP) 10 and guanosine-5′-triphosphate (GTP) 0.5 (pH 7.2 NaOH, osmolarity adjusted to 300 mosmol l^{-1} with sucrose). Tight-seal whole-cell recordings were obtained at room temperature (21–24 °C) according to Hamill *et al.* (1981). Membrane currents were recorded using a patch-clamp amplifier (EPC9, HEKA Elektronik, Lambrecht/Pfalz, Germany) and collected online with the 'TIDA for Windows' acquisition and analysis program (HEKA Elektronik). Series resistance compensation was employed to improve the voltage-clamp control (70 %) so that the maximal residual voltage error did not exceed 1 mV (Sigworth *et al.* 1995). A liquid junction potential of 10 mV was measured between the intra- and extracellular solutions and corrected online so that without correction the voltages given in this paper would be 10 mV more positive. The holding potential for most recordings was −80 mV.

Data analysis

The voltage dependence of activation and inactivation was characterised using standard protocols. The conductance (G) was calculated according to:

$$G(V) = I/(V - V_{Ca}). \quad (1)$$

The reversal potential V_{Ca} was estimated from the current–voltage (I–V) relationship, which was quite linear close to the reversal potential (values for wild-type: 27.4 ± 3.3 mV, 22.0 ± 2.9 mV and 29.1 ± 3.0 mV for CA1 neurones, dentate granule cells and neocortical neurones, respectively). The data points for the conductance G were fitted with a Boltzmann equation:

$$G/G_{max} = \frac{1}{1 + \exp[(V - V_{½})/k]}, \quad (2)$$

where G_{max} is the maximum Ca^{2+} current, $V_{½}$ is the voltage at which G is half of G_{max}, and k indicates the slope of the relationship between channel activation/inactivation and membrane voltage. This procedure was used rather than utilising the Goldman-Hodgkin-Katz equation because of the linear behaviour of I–V curves close to the reversal potential, possibly due to some contamination by activation of an outward conductance at positive voltages. Thus, data points were best fitted by the procedure described herein. It should be noted that conductances obtained using eqn (1) do not reflect the open probability of the channel population, because this would assume a linear I–V relationship of the open channel. Nevertheless, they are suitable for comparing voltage-dependent activation between groups. Data points were normalised to the maximal conductance, averaged and plotted.

The time course of deactivation of Ca^{2+} currents resistant to organic Ca^{2+} channel antagonists ($I_{Ca,R}$) was determined following brief (5 ms) test pulses to 0 mV (Cota, 1986; Randall & Tsien, 1997). From these recordings, traces obtained following complete blockade of Ca^{2+} currents by application of 1 mM Ni^{2+} were subtracted. Time constants of deactivation (τ) were extracted from the resulting traces by fitting with a double exponential function:

$$I(t) = A_0 + A_1(1 - e^{-t/\tau_1}) + A_2(1 - e^{-t/\tau_2}), \quad (3)$$

where $I(t)$ is the current amplitude at the time point t, A_1 and A_2 are the amplitudes of the first and second components, respectively, and A_0 is a constant offset. The peak of the tail currents was taken as a starting point for fitting and the relative proportions of A_0–A_2 were determined at this time point.

Concentration–response curves were plotted at the logarithmic scale and fitted with a logarithmically transformed Hill equation of the form:

$$E = E_{max} - \frac{E_{max}}{1 + 10^{(\log EC_{50} - \log c)\gamma}}, \quad (4)$$

where c is the concentration of the used substance, E_{max} the maximal possible effect, EC_{50} the concentration at which a half-maximal effect was obtained and E the effect evoked by the concentration c. γ is the Hill coefficient.

The Levenberg-Marquardt least-squares algorithm was used for all fits. Statistical analysis for significance of differences between measured variables was carried out using Student's t test with the level of significance set to < 0.05. In the case of multiple data sets, one-way ANOVA was used. Data are presented as means ± S.E.M.

RESULTS

Pharmacological isolation of Ca^{2+} currents resistant to organic Ca^{2+} channel blockers

R-type Ca^{2+} currents ($I_{Ca,R}$) are known to be present in different types of native CNS neurones, and are characterised by their resistance to organic Ca^{2+} channel antagonists (Randall & Tsien, 1995; Kavalali *et al.* 1997; Magnelli *et al.* 1998; Foehring *et al.* 2000). We analysed $I_{Ca,R}$ in dissociated CA1 pyramidal cells, dentate granule cells as well as in neocortical neurones. After establishing the whole-cell configuration of the patch-clamp technique, $I_{Ca,R}$ was isolated by pharmacologically blocking L-, P/Q- and N-type Ca^{2+} currents with saturating concentrations (Burley & Dolphin, 2000) of a combination of Ca^{2+} channel antagonists (ω-conotoxin (CgTx) GVIA (2 μM), ω-CgTx MVIIC (3 μM), ω-agatoxin (AgaTx) IVA (200 nM), nifedipine (10 μM); Fig. 1*A* and *B*). A full block of these Ca^{2+} channel components was allowed to develop for around 5 min (Fig. 1*B*). $I_{Ca,R}$ constituted 38.2 ± 17.1 % (n = 8), 15.0 ± 5.0 % (n = 5) and 21.7 ± 7.4 % (n = 6) of the total Ba^{2+} current in hippocampal CA1 neurones, dentate granule cells and neocortical neurones, respectively (test pulses to 0 mV). $I_{Ca,R}$ invariably showed a strong inactivation during the test pulse, consistent with the properties of R-type currents described previously (Foehring *et al.* 2000).

Table 1. Functional properties of Ca^{2+} currents resistant to organic Ca^{2+} channel antagonists ($I_{Ca,R}$) in hippocampal and neocortical cells in wild-type mice and $Ca_V2.3(-/-)$ mice

Parameter	CA1	Dentate gyrus	Neocortex
$Ca_V2.3(+/+)$ mice			
$V_{½,act}$ (mV)	−13.3 ± 2.7 (9)	−14.0 ± 1.8 (11)	−13.7 ± 2.1 (9)
k (mV)	8.8 ± 0.5	8.4 ± 0.7	7.2 ± 0.2
$V_{½,inact}$ (mV)	−70.3 ± 3.3 (8)	−73.1 ± 1.7 (11)	−67.8 ± 2.4 (11)
k (mV)	12.9 ± 0.6	14.8 ± 0.6	13.4 ± 0.4
Deactivation (−60 mV)			
τ_{fast} (ms)	0.297 ± 0.046 (5)	0.386 ± 0.073 (5)	0.422 ± 0.057 (5)
τ_{slow} (ms)	6.34 ± 1.08	6.19 ± 0.72	13.64 ± 3.13
$Ca_V2.3(-/-)$ mice			
$V_{½,act}$ (mV)	−25.6 ± 4.3 (7)	−23.9 ± 1.5 (7)	−20.4 ± 2.4 (8)
k (mV)	10.8 ± 1.5	9.6 ± 0.6	12.8 ± 1.3
$V_{½,inact}$ (mV)	−63.0 ± 3.9 (7)	−68.4 ± 2.6 (6)	−57.6 ± 6.5 (5)
k (mV)	13.1 ± 2.0	15.5 ± 1.7	18.9 ± 2.9

$V_{½,act}$, voltage of half-maximal activation; $V_{½,inact}$, voltage of half-maximal inactivation; k, slope factor. Numbers in parentheses indicate number of neurones. Values are given as means ± S.E.M.

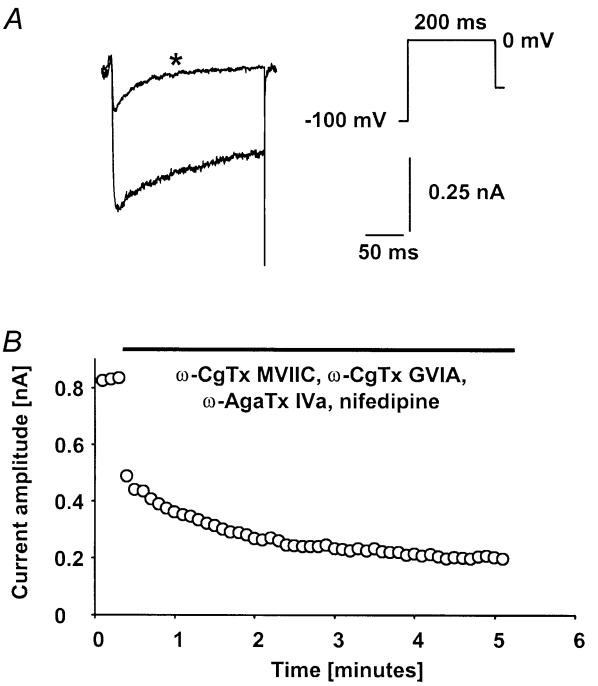

Figure 1. Pharmacological isolation of Ca^{2+} currents resistant to organic Ca^{2+} channel antagonists ($I_{Ca,R}$) by combined application of ω-conotoxin (CgTx) GVIA (2 μM), ω-CgTx MVIIC (3 μM), ω-agatoxin (AgaTx) IVa (200 nM) and nifedipine (10 μM) in wild-type mice

A, Ba^{2+} currents were elicited with voltage jumps to 0 mV (200 ms) following a conditioning prepulse to −100 mV (2 s, see inset). The holding potential in this recording was −50 mV. The current trace following the saturation of the block is marked with an asterisk. *B*, time course of block of the peak Ba^{2+} current by combined application of the Ca^{2+} channel antagonists (horizontal bar). Care was always taken to ensure that the block was saturated before analysis of $I_{Ca,R}$ current properties.

Contribution of $Ca_V2.3$ subunits to $I_{Ca,R}$ in CA1 pyramidal neurones, dentate granule cells and neocortical neurones

To determine which portion of $I_{Ca,R}$ is mediated by $Ca_V2.3$ subunits, the properties of Ba^{2+} currents in mice lacking expression of the $Ca_V2.3$ subunit (Fig. 2*A*) were examined. As shown in Fig. 2*B*, the amplitude of $I_{Ca,R}$ elicited with voltage steps to −10 mV was markedly decreased in $Ca_V2.3$-deficient mice. In CA1 neurones, the current amplitude normalised to cell capacitance was 20.4 ± 3.9 pA pF^{-1} ($n = 9$) in wild-type and 4.3 ± 1.3 pA pF^{-1} ($n = 10$) in $Ca_V2.3$-deficient animals, corresponding to a 79 % decrease (Fig. 2*B*, left-most panels, Fig. 2*Ca*). In neocortical neurones, a more pronounced decrease of 87 % was noted from 25.1 ± 5.3 ($n = 9$) to 3.4 ± 0.9 pA pF^{-1} ($n = 9$; Fig. 2*B*, right-most panels, Fig. 2*Ca*). In contrast, $I_{Ca,R}$ in dentate granule cells was less affected in $Ca_V2.3$-deficient mice (12.2 ± 2.3 pA pF^{-1}, $n = 12$ in wild-type and 6.5 ± 1.6 pA pF^{-1} in $Ca_V2.3$-deficient mice, $n = 7$, 47 % decrease, Fig. 2*B* and *Ca*). Thus, $I_{Ca,R}$ in CA1 and neocortical neurones was mediated mostly by $Ca_V2.3$ subunits, with a smaller contribution in dentate granule cells. We also assessed the amplitude of the compound current consisting of L-, N- and P/Q-type currents by quantifying the current component blocked by co-application of ω-CgTx GVIA and MVIIC, ω-AgaTx IVA and nifedipine. In contrast to $I_{Ca,R}$, this current component was unaltered in $Ca_V2.3$-deficient mice (Fig. 2*Cb*).

Selective reduction of a rapidly deactivating, putative R-type Ca^{2+} current in $Ca_V2.3$-deficient mice

The somatodendritic $I_{Ca,R}$ is composed of an R-type, as well as a smaller T-type component (Fisher *et al.* 1990). We have therefore addressed the question of whether only

R-type or both of these components are reduced in $Ca_V2.3$-deficient mice. In order to discriminate R- and T-type components, we have made use of the fact that the deactivation time course of R-type current components is markedly faster than that of T-type currents (Randall & Tsien, 1997). We have therefore fitted the deactivation time course of $I_{Ca,R}$ following brief (5 ms) depolarisations that activate both R- and T-type currents (Fig. 3*A*, inset) with a sum of two exponential functions. This protocol allowed the discrimination of a rapidly deactivating, putative R-type component from a slowly deactivating, putative T-type component (Cota, 1986; Randall & Tsien, 1997). At a potential of −60 mV, a faster time constant in the range of 300–400 μs and a slower time constant in the

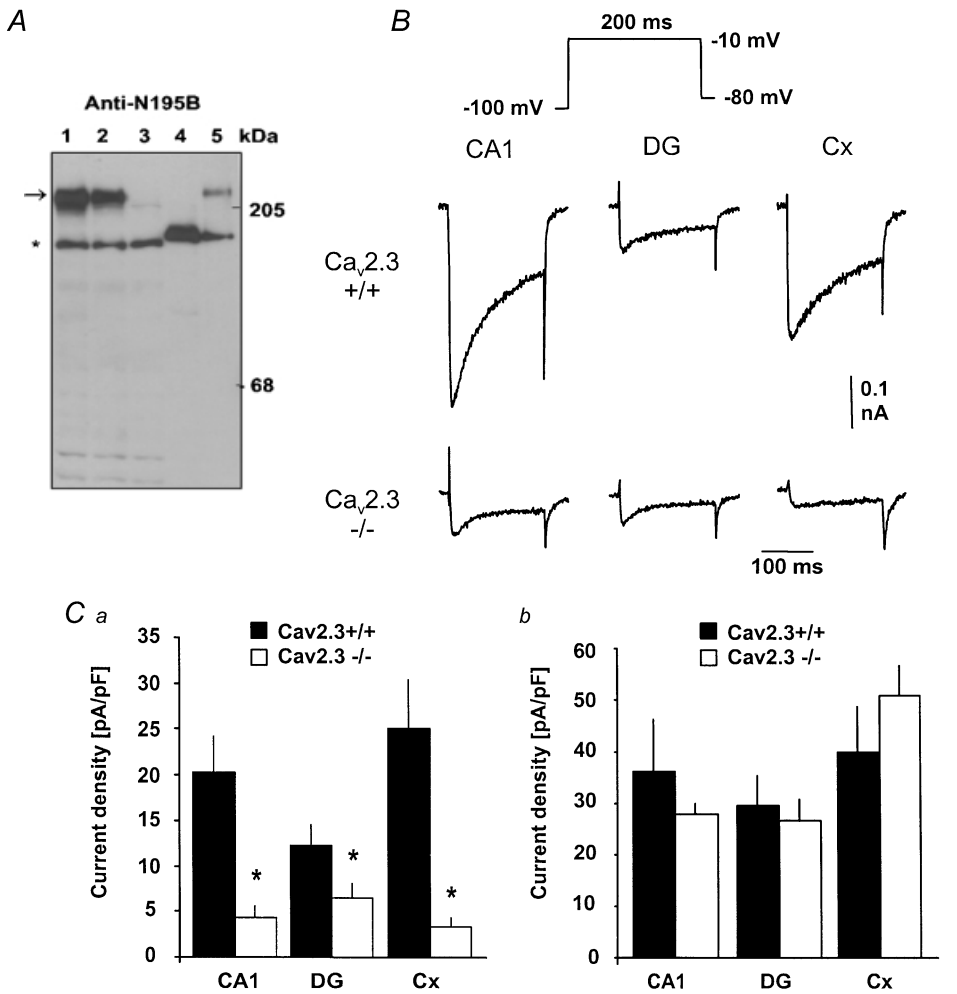

Figure 2. $I_{Ca,R}$ is considerably reduced in $Ca_V2.3$(−/−) mice

A, analysis of $Ca_V2.3$ protein levels using Western blot analysis of microsomal membrane proteins. Microsomes (24 μg) were isolated from the brains of wild-type mice (lane 1), from heterozygous litter mates (lane 2) and from $Ca_V2.3$ null mutants (lane 3). Microsomal membranes from untransfected (lane 4; 5 μg) and stably transfected with $Ca_V2.3$ human embryonic kidney (HEK)-293 cells (lane 5; 2 μg) were used as negative and positive controls, respectively. The primary antibody (Anti-N195B) is directed against an epitope of $Ca_V2.3$ common to all known $Ca_V2.3$ splice variants. A polypeptide of 246 kDa ($Ca_V2.3$) was detected in wild-type and heterozygous mice as well as in stably transfected HEK-293 cells (arrow). No staining was observed at this position in $Ca_V2.3$ null mutant mice or untransfected HEK-293 cells (lanes 3 and 4). Unspecific staining was detected as a faint band at 205 kDa and a major band (*), neither of which is related to $Ca_V2.3$ because they were also detected after preabsorption of the serum by the antigenic peptide (not shown). *B*, $I_{Ca,R}$ in CA1 pyramidal neurones (CA1), dentate granule cells (DG) and neocortical neurones (Cx) in both wild-type (upper traces) and $Ca_V2.3$-deficient mice (lower traces). $I_{Ca,R}$ was elicited with the voltage-step protocol shown in the inset. Calibration bars apply to all traces. *Ca*, the amplitude of $I_{Ca,R}$ elicited with the voltage step to −10 mV was significantly (*$P < 0.05$) decreased in $Ca_V2.3$-deficient mice (open bars) compared to wild-type mice (filled bars) in all cell types studied. The amplitude of $I_{Ca,R}$ elicited with command pulses to −10 mV was normalised to cell capacitance. *Cb*, normalised amplitude of the current component blocked by the combination of Ca^{2+} channel antagonists used to isolate $I_{Ca,R}$ (see Fig. 1*A*). No difference between wild-type mice and mice lacking $Ca_V2.3$ subunits was detected.

range of 6–10 ms could be observed (see Table 1 for values). The faster component (filled bars, Fig. 3*B*) comprised the main portion of tail current decay in wild-type mice (90.2 ± 2.3, 62.4 ± 9.7 and 85.8 ± 3.7 % for CA1 neurones, dentate granule cells and neocortical neurones, respectively, at −60 mV; compare Fig. 3*Ba* and *Bb*, $n = 5$ for all measurements; Thompson & Schwindt, 1991; Foehring *et al.* 2000). In mice lacking $Ca_V2.3$ subunits, the time constants of both components were not significantly changed. However, the amplitude contribution of the rapidly decaying, putative R-type component was markedly reduced (by 90.4 %, 76.6 % and 90.9 % for CA1 neurones, dentate granule cells and neocortical neurones, respectively; $n = 5$ for all measurements, $P < 0.05$, Fig. 3*Ba*). In contrast, the more slowly decaying, putative T-type component remained unaffected in CA1 and cortical neurones (Fig. 3*Bb*). Some reduction in this component was observed in dentate granule cells from $Ca_V2.3$ knockout mice ($P < 0.05$), but to a significantly lower degree than the reduction in the rapidly decaying component ($P < 0.05$, compare Fig. 3*Ba* and *Bb*). Taken together, these results suggest that genetic deletion of $Ca_V2.3$ subunits selectively affects R-type Ca^{2+} currents in cortical and CA1 neurones.

Voltage dependence of $I_{Ca,R}$ in wild-type and $Ca_V2.3(-/-)$ mice

Next, we analysed the voltage-dependent activation and inactivation behaviour of $I_{Ca,R}$ in CA1 pyramidal cells, dentate granule cells, and neocortical cells in wild-type

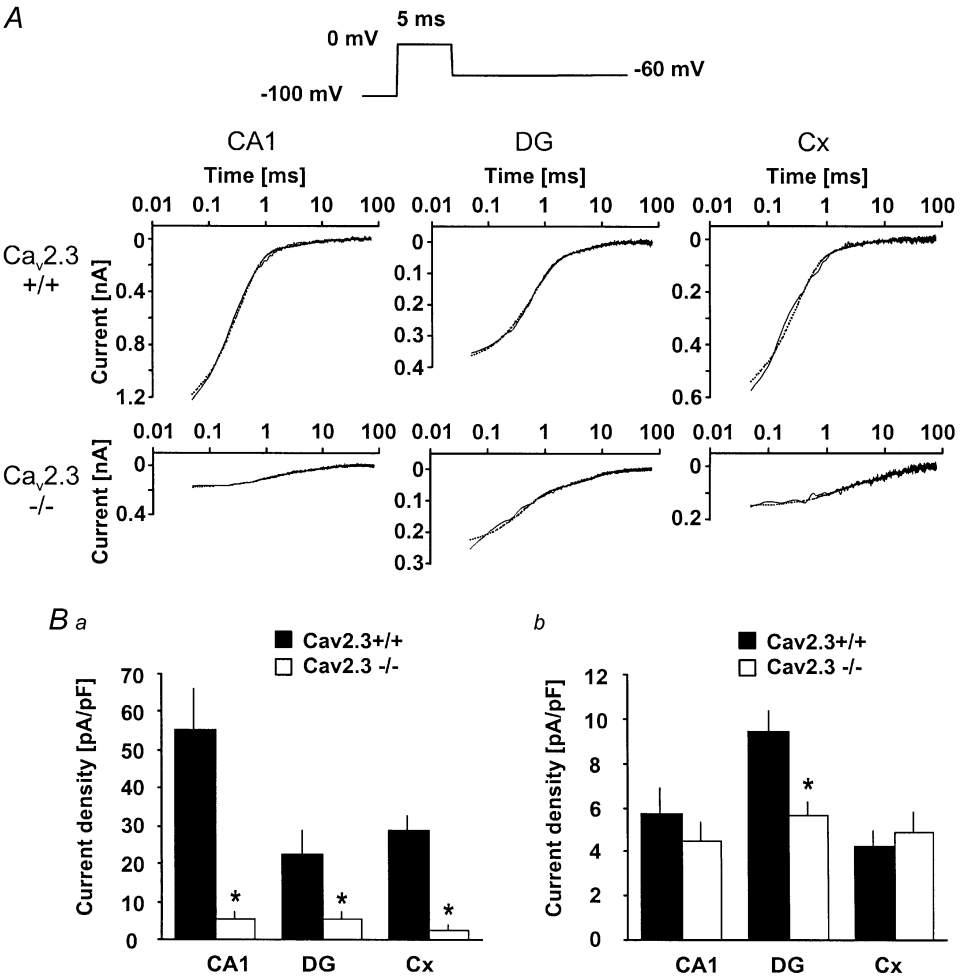

Figure 3. Selective reduction of a rapidly deactivating, putative R-type current in $Ca_V2.3(-/-)$ mice

A, deactivation kinetics were determined following a brief (5 ms) test pulse following a conditioning prepulse to −100 mV (see inset). The holding potential for these recordings was −80 mV. Recordings shown on a semilogarithmic scale were generated by subtracting traces obtained after complete blockade of inward currents with 1 mM Ni^{2+}. The resulting Ba^{2+} current tails were fitted with a biexponential function shown as a dashed line superimposed on representative example traces. Traces are shown beginning from the peak amplitude. Averaged time constants are given in Table 1. *B*, the amplitude contributions of the fast- (*Ba*) and the slowly deactivating components (*Bb*) were derived from the fits, normalised to the cell capacitance and averaged in wild-type (filled bars) and $Ca_V2.3$-deficient mice (open bars). The rapidly decaying, putative R-type component was considerably reduced in $Ca_V2.3$-deficient mice (*$P < 0.05$).

mice (see example traces in Fig. 4*Aa* and *Ab*) and mice lacking $Ca_V2.3$ subunits (Fig. 4*Ba* and *Bb*) using the voltage protocols shown in the insets. In wild-type mice, this analysis yielded similar voltages of half-maximal activation and inactivation for CA1 pyramidal cells ($n = 8$, Fig. 4*C*, filled squares), dentate granule neurones ($n = 11$, Fig. 4*D*, filled circles) and neocortical neurones ($n = 11$, Fig. 4*E*, filled triangles, see also Table 1). These values were in good agreement with the properties of cloned $Ca_V2.3$ channels, and R-type currents in native neurones (Ellinor *et al.* 1993; Randall & Tsien, 1997; Nakashima *et al.* 1998; Pereverzev *et al.* 1998; Foehring *et al.* 2000; Magistretti *et al.* 2000).

In $Ca_V2.3$-deficient mice, a more hyperpolarised threshold of activation was observed in all cell types (Fig. 4*C–E*). Correspondingly, the voltage of half-maximal activation was significantly ($P < 0.05$) shifted in a hyperpolarising direction in CA1 neurones ($n = 7$, Fig. 4*C*, open squares) and dentate granule neurones ($n = 7$, Fig. 4*D*, open circles).

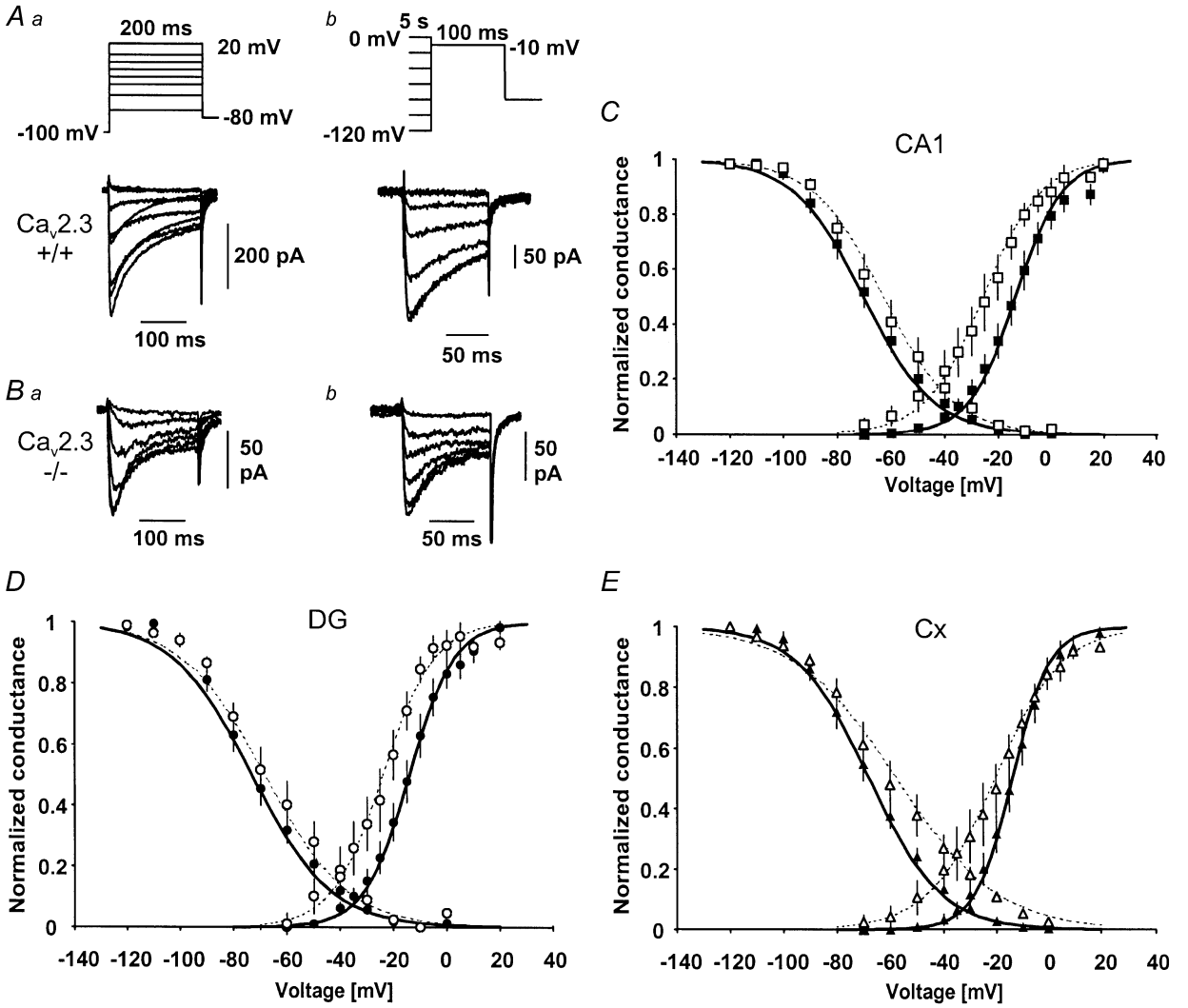

Figure 4. Voltage dependence of $I_{Ca,R}$ in wild-type and $Ca_V2.3$-deficient mice

A, voltage dependence of activation (*Aa*) and inactivation (*Ab*) in a CA1 neurone from a wild-type mouse. The activation behaviour was analysed with voltage jumps to various command voltages (200 ms) following a conditioning prepulse to −100 mV (2 s, see inset). Inactivation was induced with a 5 s conditioning pulse to various voltages followed by a test pulse to −10 mV (50 ms, see inset). *B*, voltage dependence of activation (*Ba*) and inactivation (*Bb*) in a CA1 neurone from a $Ca_V2.3$-deficient mouse. *C*, *D*, *E*, voltage-dependent activation and inactivation behaviour for wild-type mice (filled symbols) and $Ca_V2.3$-deficient mice (open symbols) in CA1 neurones (*C*), dentate granule neurones (DG, *D*) and cortical neurones (Cx, *E*). Data points for the steady-state activation curve were obtained by calculating the conductance from peak Ba^{2+} current values (see *Aa*, *Ba*), and plotting normalised and averaged values *vs.* the command voltage. The inactivation curve was constructed from normalised and averaged peak conductances and plotted *vs.* the voltage of the conditioning pulse. Boltzmann functions were fitted to the data points using the Levenberg-Marquardt least-squares algorithm and are shown superimposed on the data points. The half-maximal activation and inactivation voltages averaged across individual experiments are given in Table 1.

In cortical neurones, the voltage of half-maximal activation ($n = 8$, Fig. 4*E*, open triangles, see also Table 1) was not significantly different compared to wild-type mice ($P = 0.052$). The inactivation curves did not differ in mice lacking $Ca_V2.3$ subunits and wild-type mice (Fig. 4*C–E*). The more hyperpolarised threshold of activation and voltage of half-maximal activation is consistent with a higher contribution of T-type Ca^{2+} currents to the compound current $I_{Ca,R}$ in $Ca_V2.3$-deficient mice. Such a higher contribution would be expected as a consequence of a selective reduction of R-type Ca^{2+} currents (see Fig. 3). The lack of significant changes in the inactivation behaviour is most probably explained by rather similar properties of voltage-dependent inactivation of R-type/$Ca_V2.3$ and T-type currents (Randall & Tsien, 1997; Klöckner *et al.* 1999), especially if $Ca_V2.3$ subunits are coexpressed with accessory subunits (Stephens *et al.* 1997).

Pharmacological properties of $I_{Ca,R}$

Recombinant $Ca_V2.3$ channels show distinctive pharmacological properties. For instance, $Ca_V2.3$-mediated Ca^{2+} currents in expression systems were shown to be sensitive to nanomolar concentrations of the spider toxin SNX-482 (Tottene *et al.* 2000; Vajna *et al.* 2001). Application of various concentrations of SNX-482 in wild-type mice

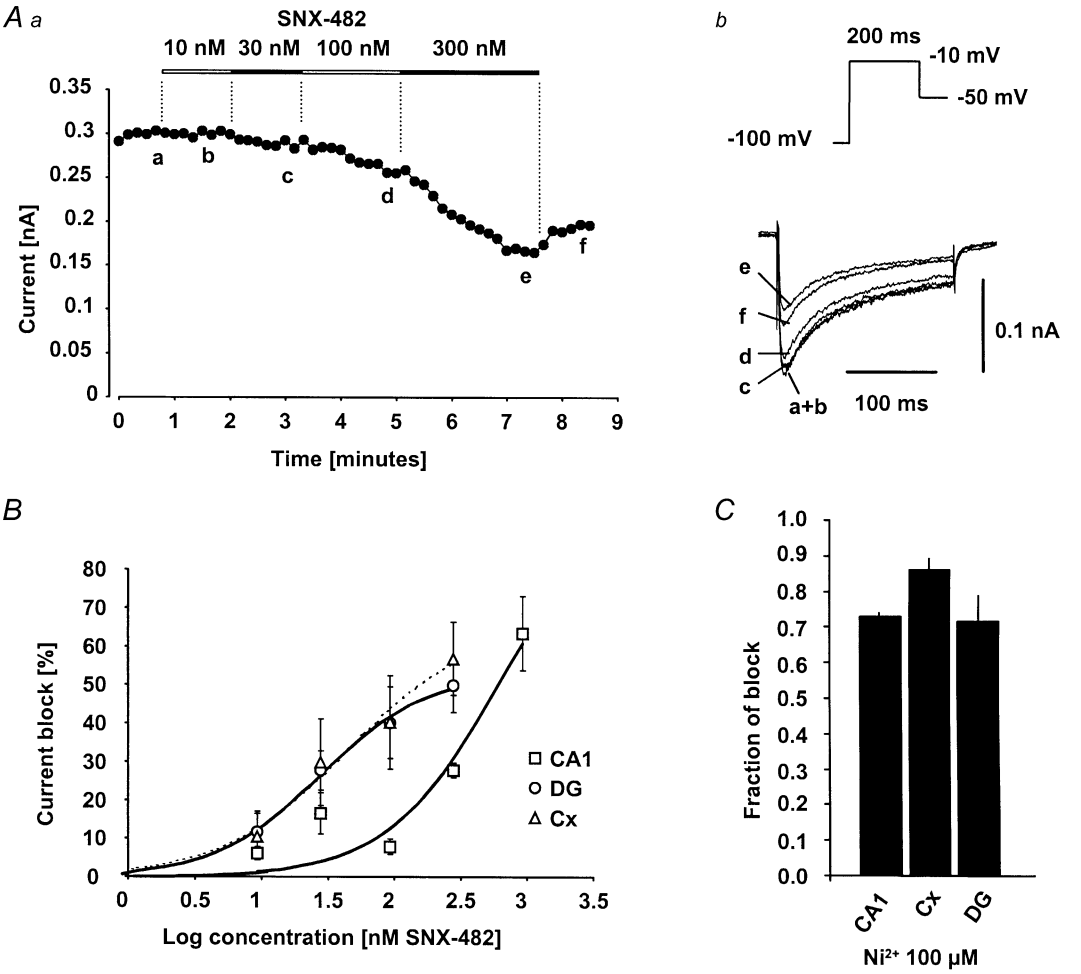

Figure 5. Pharmacological properties of $I_{Ca,R}$

A, time course of a representative experiment during application of 10–300 nM SNX-482 (*Aa*, see bars for duration of application). The amplitude of $I_{Ca,R}$ in a cortical neurone from a wild-type mouse is depicted over time. Current traces elicited at the time points indicated by the lower-case letters are shown in panel *Ab*. The voltage step is shown in the inset and was applied following a 2 s hyperpolarising prepulse to −100 mV. The holding potential in all pharmacological experiments was −50 mV. *B*, concentration dependence of $I_{Ca,R}$ block by SNX-482 in CA1 neurones (squares), dentate granule cells (circles) and cortical neurones (triangles) in wild-type mice. Data points were fitted with the logarithmically transformed Hill equation (eqn (4), see Methods) and the fitted curves are superimposed on the data points (dashed curve: cortex). The fitted curve for CA1 neurones is given for illustrative purposes only. Note that block by SNX-482 does not seem to saturate completely during some applications, either due to a slow onset of the block, or to some degree of unavoidable rundown. *C*, fraction of Ba^{2+} current blocked by application of 100 μM Ni^{2+} in the different neurone types from wild-type mice.

(10, 30, 100 and 300 nM, Fig. 5*A*) led to a pronounced concentration-dependent reduction of $I_{Ca,R}$ in cortical neurones and dentate granule neurones (block of 56.9 ± 9.4 %, $n = 4$ and 50.0 ± 7.0 %, $n = 4$, respectively, 300 nM SNX-482). The data points were fitted with the logarithmically transformed Hill equation (eqn (4), see Methods, EC_{50} 30 and 47 nM, maximal block E_{max} 65.5 and 53.1 %, Hill coefficient 1.09 and 0.93 for cortical neurones and dentate granule neurones, respectively). The $I_{Ca,R}$ in CA1 neurones proved to be significantly less sensitive to SNX-482 (block of 27.9 ± 1.9 %, $n = 7$, 300 nM SNX-482), as suggested previously (Newcomb *et al.* 1998). Pronounced block of $I_{Ca,R}$ was only observed at very high concentrations of SNX-482 (1 μM), which are thought to exert unspecific effects (Neelands *et al.* 2000; Bourinet *et al.* 2001) and did not saturate in this concentration range. For this reason, the values obtained for CA1 neurones with fitting as above were considered unreliable.

In mice lacking $Ca_V2.3$ channels, it proved difficult to examine the pharmacology of $I_{Ca,R}$ due to the small amplitude of this residual current. We did succeed in obtaining a limited number of recordings in which the effects of SNX-482 on $I_{Ca,R}$ could be assessed in dentate granule neurones (1 μM SNX-482, $n = 2$) and CA1 neurones (1 μM, $n = 2$; 300 nM SNX-482, $n = 5$). The portion of $I_{Ca,R}$ blocked by SNX-482 was markedly reduced in CA1 neurones from $Ca_V2.3(-/-)$ mice (300 nM: from 2.1 ± 0.2 to 0.7 ± 0.1 pA pF^{-1}, $P < 0.05$; 1 μM: 4.7 ± 0.8 to 0.4 pA pF^{-1}). Likewise, in dentate granule cells, the SNX-482-sensitive component amounted to 3.3 ± 0.8 pA pF^{-1} (300 nM), while only 1.2 pA pF^{-1} was blocked in $Ca_V2.3(-/-)$ mice, even at a blocker concentration of 1 μM. Even though these results show that the SNX-482-sensitive portion of $I_{Ca,R}$ is reduced in mice lacking $Ca_V2.3$, they also suggest effects of SNX-482 on channels other than $Ca_V2.3$. Indeed, we found that application of 300 nM SNX-482 onto CA1 neurones from mice lacking $Ca_V2.3$ subunits results in a modest but significant block of the total whole-cell Ca^{2+} current (16.1 ± 4.9 % block, $n = 4$). These effects were not further analysed, but demonstrate that SNX-482 does not exclusively block $Ca_V2.3$ currents at these concentrations, as suggested previously by other studies (Neelands *et al.* 2000; Bourinet *et al.* 2001).

$Ca_V2.3$ Ca^{2+} channels are also highly sensitive to the divalent cation Ni^{2+} (Ellinor *et al.* 1993), even though Ni^{2+} is not specific for these channels (Zhang *et al.* 1993; Soong *et al.* 1993; Pereverzev *et al.* 1998). In wild-type mice, Ni^{2+} (100 μM) potently inhibited $I_{Ca,R}$ in all cell types under investigation (CA1 neurones: 73.0 ± 1.1 %, $n = 5$; neocortical cells: 86.0 ± 3.2 %, $n = 6$; and dentate granule cells: 71.4 ± 7.4 %, $n = 5$, Fig. 5*B*). In $Ca_V2.3$-deficient mice, $I_{Ca,R}$ also proved to be sensitive to 100 μM Ni^{2+} in all cell types under investigation (CA1 neurones: 62.3 ± 4.9 % block, $n = 5$, neocortical cells: 74.0 ± 0.8 % block, $n = 4$; and dentate granule cells: 89.0 ± 11.1 % block, $n = 4$), possibly due to the Ni^{2+} sensitivity of some T-type channel subunits (Lee *et al.* 1999*b*).

DISCUSSION

Voltage-dependent Ca^{2+} channels constitute a major link between neuronal excitability and intracellular Ca^{2+}. Therefore, the question of which Ca^{2+} channel subunits underlie these currents in native neurones has been a subject of intensive research. For some Ca^{2+} channel α_1 subunits, specific antagonists have permitted the dissection of their contribution to Ca^{2+} currents in native cells. In the case of R- and T-type Ca^{2+} currents, the lack of specific antagonists has necessitated the use of antisense (Piedras-Renteria *et al.* 1997; Lambert *et al.* 1998; Piedras-Renteria & Tsien, 1998; Tottene *et al.* 2000) or transgenic strategies (Wilson *et al.* 2000; Lee *et al.* 2002) to ablate the expression of specific α_1 subunits. R-type currents resistant to organic Ca^{2+} channel antagonists ($I_{Ca,R}$) can be found in most neurones, such as neocortical and striatal neurones (Foehring *et al.* 2000), CA1 neurones (Ishibashi *et al.* 1995), dentate granule cells (Eliot & Johnston, 1994; Beck *et al.* 1998) and cerebellar granule neurones (Forti *et al.* 1994; Tottene *et al.* 1996, 2000; Schramm *et al.* 1999). They have also been recorded from the insulinoma cell line INS-1 and show a moderate sensitivity towards SNX-482 (Vajna *et al.* 2001). Nevertheless, the molecular basis of these currents has remained unknown. In the present study, knock-out mice lacking the $Ca_V2.3$ Ca^{2+} channel subunit were used to investigate whether this subunit underlies R-type Ca^{2+} currents in different types of central neurones known to express $Ca_V2.3$ mRNA (Soong *et al.* 1993; Hendriksen *et al.* 1997; Foehring *et al.* 2000). Neocortical and CA1 pyramidal neurones, as well as hippocampal dentate granule cells were analysed, all of which expressed Ca^{2+} currents resistant to organic Ca^{2+} channel antagonists, $I_{Ca,R}$, with properties reminiscent of cloned $Ca_V2.3$ subunits (see also Foehring *et al.* 2000). Experiments in mice lacking $Ca_V2.3$ subunits show unequivocally that this subunit underlies the major portion of $I_{Ca,R}$ in CA1 and neocortical neurones (~79 and 87 %), and a smaller fraction of this current in dentate granule neurones (~47 %). Furthermore, our analyses of tail currents show a specific reduction of a rapidly deactivating, putative R-type current in mice lacking $Ca_V2.3$ subunits, with no (in CA1, cortical cells) or significantly less (in dentate granule cells) effects on a small, slowly deactivating putative T-type current component (Klöckner *et al.* 1999). The selective reduction of R-type currents in $Ca_V2.3$ mice would be expected to cause an increased contribution of T-type currents to $I_{Ca,R}$ in these animals, consistent with the more hyperpolarised voltage-dependent activation curve we observed in $Ca_V2.3(-/-)$ mice.

Molecular basis of $I_{Ca,R}$ in other cell types

Hitherto, two studies have addressed the question of the molecular basis of R-type currents using either antisense knockdown (Tottene *et al.* 2000) or transgenic techniques (Wilson *et al.* 2000). The former study demonstrated, similar to our study, that $Ca_V2.3$ subunits underlie a major portion of R-type currents in cerebellar granule cell cultures (Tottene *et al.* 2000). This is unlike findings in cerebellar granule cell and dorsal root ganglion cell cultures from mice lacking the $Ca_V2.3$ subunit, in which only a minor portion of the R-type current seems to be due to the expression of $Ca_V2.3$ (Wilson *et al.* 2000). There may be several reasons for these discrepancies. For instance, in the pharmacological isolation used by Wilson *et al.* the concentration of ω-agatoxin IVA used (200 nM) may have been insufficient for a complete block of Q-type components (half-blocking concentration ~90 nM in cerebellar granule cells, see Randall & Tsien, 1995), resulting in a contribution of such currents to the putative R-type current. In our study, as well as in the study by Tottene *et al.* addition of ω-conotoxin MVIIC most probably allowed us to avoid contamination of R-type currents by Q-type components. Alternatively, it may be possible that either T-type channel subunits (especially in dorsal root ganglion neurones, see Lovinger & White, 1989; Hilaire *et al.* 1997), or as yet uncloned subunits, giving rise to blocker-resistant currents may underlie part of the putative R-type current under the specific culture conditions chosen by Wilson *et al.* (2000). Nevertheless, these contrasting observations may also reflect a molecular diversity of R-type currents in the central nervous system.

Pharmacological properties of $I_{Ca,R}$ in central neurones

The specific pharmacological properties common to most of the isoforms of $Ca_V2.3$ studied so far include a high sensitivity to Ni^{2+} blockade (Soong *et al.* 1993), but this substance may also block other Ca^{2+} channels at relatively low concentrations (Zhang *et al.* 1993; Schneider *et al.* 1994; Williams *et al.* 1994). To date, the peptide neurotoxin SNX-482 is thought to be the only selective, high-affinity antagonist targeting $Ca_V2.3$ channels (Newcomb *et al.* 1998; Tottene *et al.* 2000). On the basis of their sensitivity to the spider toxin SNX-482, three components of the R-type current were distinguished in cultured cerebellar granule cells (Tottene *et al.* 2000). Two of these components are completely blocked by 100 nM SNX-482. A third component was only blocked at very high concentrations of SNX-482, which also affect other current components (Newcomb *et al.* 1998; Tottene *et al.* 2000).

Our results also suggest that $Ca_V2.3$ subunits give rise to both SNX-482-sensitive and SNX-482-resistant components of $I_{Ca,R}$. In CA1 neurones, $Ca_V2.3$ subunits underlie 80–90 % of $I_{Ca,R}$, but only around 50 % of this current is blocked by high (300 nM) concentrations of SNX-482, suggesting that the remainder of the $Ca_V2.3$-mediated current corresponds to the relatively SNX-482 resistant current component observed in cerebellar granule neurones (Tottene *et al.* 2000). In dentate granule neurones, $Ca_V2.3$ subunits underlie only part (~50 %) of $I_{Ca,R}$. A large part of this component appeared to be blocked by 300 nM SNX-482. Thus, our results suggest both that $Ca_V2.3$ subunits may give rise to Ca^{2+} currents with differing SNX-482 sensitivity, and that the relative contribution of these components may vary from cell type to cell type.

Possible molecular basis for the diversity of $Ca_V2.3$-mediated Ca^{2+} currents in native neurones

Taken together, the results of the present study and other published data suggest that the biophysical and pharmacological properties of R-type currents in native neurones are diverse, even in those cases where antisense or transgenic approaches have confirmed the molecular identity of the channel protein. One explanation for this variation could be the expression of different $Ca_V2.3$ splice variants in different neurone types. At least six different splice forms, varying in the II–III loop and the C-terminus, can be deduced from RT-PCR studies (Marubio *et al.* 1996; Vajna *et al.* 1998; Schramm *et al.* 1999). Some of these show a differential expression pattern during development and in the mature brain (Pereverzev *et al.* 1998; Schramm *et al.* 1999). However, the biophysical and pharmacological properties of these C-terminal splice variants are quite similar (Pereverzev *et al.* 1998; Schramm *et al.* 1999), and in particular both variants are sensitive to SNX-482 when expressed in human embryonic kidney (HEK)-293 cells. It has been suggested that the binding site for the peptide toxin could be occluded by an auxiliary subunit (Newcomb *et al.* 1998), but coexpression of the human α_{1Ed} subunit with two auxiliary subunits, human β_3 or $\alpha_2\delta_2$, did not influence inward currents in HEK-293 cells (Vajna *et al.* 2001).

In summary, our study shows unequivocally that a large part of the R-type current in the central neurone types we have investigated is carried by $Ca_V2.3$ subunits. Taken together with published data on $Ca_V2.3$-mediated currents in native cells (Tottene *et al.* 2000), our results indicate that $Ca_V2.3$ subunits may underlie R-type currents with different functional properties. In view of the importance of the $Ca_V2.3$ subunit in pain responses and spatial memory (Saegusa *et al.* 2000; Kubota *et al.* 2001), future studies should address the molecular basis for this intriguing functional diversity.

REFERENCES

Beck, H., Steffens, R., Heinemann, U. & Elger, C. E. (1998). Properties of voltage-activated calcium currents in acutely dissociated human hippocampal granule cells. *Journal of Neurophysiology* **77**, 1526–1537.

Birnbaumer, L., Campbell, K. P., Catterall, W. A., Harpold, M. M., Hofmann, F., Horne, W. A., Mori, Y., Schwartz, A., Snutch, T. P., Tanabe, T. *et al.* (1994). The naming of voltage-gated calcium channels. *Neuron* **13**, 505–506.

Bourinet, E., Stotz, S. C., Spaetgens, R. L., Dayanithi, G., Lemos, J., Nargeot, J. & Zamponi, G. W. (2001). Interaction of SNX482 with domains III and IV inhibits activation gating of alpha1E ($Ca_V2.3$). calcium channels. *Biophysical Journal* **81**, 79–88.

Burley, J. R. & Dolphin, A. C. (2000). Overlapping selectivity of neurotoxin and dihydropyridine calcium channel blockers in cerebellar granule neurones. *Neuropharmacology* **39**, 1740–1755.

Cota, G. (1986). Calcium channel currents in pars intermedia cells of the rat pituitary gland. Kinetic properties and washout during intracellular dialysis. *Journal of General Physiology* **88**, 83–105.

Cribbs, L. L., Lee, J. H., Yang, J., Satin, J., Zhang, Y., Daud, A., Barclay, J., Williamson, M. P., Fox, M., Rees, M. & Perez-Reyes, E. (1998). Cloning and characterization of alpha1H from human heart, a member of the T-type Ca^{2+} channel gene family. *Circulation Research* **83**, 103–109.

Eliot, L. S. & Johnston, D. (1994). Multiple components of calcium current in acutely dissociated dentate gyrus granule neurones. *Journal of Neurophysiology* **72**, 762–777.

Ellinor, P. T., Zhang, J.-F., Randall, A. D., Zhou, M., Schwarz, T. L., Tsien, R. W. & Horne, W. A. (1993). Functional expression of a rapidly inactivating neuronal calcium channel. *Nature* **363**, 455–458.

Ertel, E. A., Campbell, K. P., Harpold, M. M., Hofmann, F., Mori, Y., Perez-Reyes, E., Schwartz, A., Snutch, T. P., Tanabe, T., Birnbaumer, L., Tsien, R. W. & Catterall, W. A. (2000). Nomenclature of voltage-gated calcium channels. *Neuron* **25**, 533–535.

Fisher, R. E., Gray, R. & Johnston, D. (1990). Properties and distribution of single voltage-gated calcium channels in adult hippocampal neurons. *Journal of Neurophysiology* **64**, 91–104.

Flockerzi, V., Oeken, H. J. & Hofmann, F. (1986). Purification of a functional receptor for calcium-channel blockers from rabbit skeletal-muscle microsomes. *European Journal of Biochemistry* **161**, 217–224.

Foehring, R. C., Mermelstein, P. G., Song, W. J., Ulrich, S. & Surmeier, D. J. (2000). Unique properties of R-type calcium currents in neocortical and neostriatal neurons. *Journal of Neurophysiology* **84**, 2225–2236.

Forti, L., Tottene, A., Moretti, A. & Pietrobon, D. (1994). Three novel types of voltage-dependent calcium channels in rat cerebellar neurons. *Journal of Neuroscience* **14**, 5243–5256.

Hamill, O. P., Marty, A., Neher, E., Sakmann, B. & Sigworth, F. J. (1981). Improved patch-clamp techniques for high-resolution current recording from cells and cell-free membrane patches. *Pflügers Archiv* **391**, 85–100.

Hendriksen, H., Kamphuis, W. & Lopes Da Silva, F. H. (1997). Changes in voltage-dependent calcium channel alpha1-subunit mRNA levels in the kindling model of epileptogenesis. *Brain Research. Molecular Brain Research* **50**, 257–266.

Hilaire, C., Diochot, S., Desmadryl, G., Richard, S. & Valmier, J. (1997). Toxin-resistant calcium currents in embryonic mouse sensory neurons. *Neuroscience* **80**, 267–276.

Hofmann, F., Lacinova, L. & Klugbauer, N. (1999). Voltage-dependent calcium channels: from structure to function. *Reviews of Physiology, Biochemistry and Pharmacology* **139**, 33–87.

Ishibashi, H., Rhee, J. S. & Akaike, A. (1995). Regional difference of high voltage-activated Ca^{2+} channels in rat CNS neurones. *NeuroReport* **6**, 1621–1624.

Kavalali, E. T., Zhuo, M., Bito, H. & Tsien, R. W. (1997). Dendritic Ca^{2+} channels characterized by recordings from isolated hippocampal dendritic segments. *Neuron* **18**, 651–663.

Klöckner, U., Lee, J. H., Cribbs, L. L., Daud, A., Hescheler, J., Pereverzev, A., Perez-Reyes, E. & Schneider, T. (1999). Comparison of the Ca^{2+} currents induced by expression of three cloned alpha1 subunits, alpha1G, alpha1H and alpha1I, of low-voltage-activated T-type Ca^{2+} channels. *European Journal of Neuroscience* **11**, 4171–4178.

Kubota, M., Murakoshi, T., Saegusa, H., Kazuno, A., Zong, S., Hu, Q., Noda, T. & Tanabe, T. (2001). Intact LTP and fear memory but impaired spatial memory in mice lacking $Ca_V2.3$ (alpha1E). channel. *Biochemical and Biophysical Research Communications* **282**, 242–248.

Lambert, R. C., McKenna, F., Maulet, Y., Talley, E. M., Bayliss, D. A., Cribbs, L. L., Lee, J. H., Perez-Reyes, E. & Feltz, A. (1998). Low-voltage-activated Ca^{2+} currents are generated by members of the Ca_VT subunit family (α1G/H). in rat primary sensory neurons. *Journal of Neuroscience* **18**, 8605–8613.

Lee, J. H., Daud, A. N., Cribbs, L. L., Lacerda, A. E., Pereverzev, A., Klöckner, U., Schneider, T. & Perez-Reyes, E. (1999*a*). Cloning and expression of a novel member of the low voltage-activated T-type calcium channel family. *Journal of Neuroscience* **19**, 1912–1921.

Lee, J. H., Gomora, J. C., Cribbs, L. L. & Perez-Reyes, E. (1999*b*). Nickel block of three cloned T-type calcium channels: low concentrations selectively block alpha1H. *Biophysical Journal* **77**, 3034–3042.

Lee, S. C., Choi, S., Lee, T., Kim, H. L., Chin, H. & Shin, H. S. (2002). Molecular basis of R-type calcium channels in central amygdala neurons of the mouse. *Proceedings of the National Academy of Sciences of the USA* **99**, 3276–3281.

Lovinger, D. M. & White, G. (1989). Post-natal development of burst firing behavior and the low-threshold transient calcium current examined using freshly isolated neurons from rat dorsal root ganglia. *Neuroscience Letters* **102**, 50–57.

Magistretti, J., Brevi, S. & De Curtis, M. (2000). A blocker-resistant, fast-decaying, intermediate-threshold calcium current in palaeocortical pyramidal neurons. *European Journal of Neuroscience* **12**, 2376–2386.

Magnelli, V., Baldelli, P. & Carbone, E. (1998). Antagonist-resistant calcium currents in rat embryo motoneurons. *European Journal of Neuroscience* **10**, 1810–1825.

Marubio, L. M., Roenfeld, M., Dasgupta, S., Miller, R. J. & Philipson, L. H. (1996). Isoform expression of the voltage-dependent calcium channel alpha1E. *Receptors and Channels* **4**, 243–251.

Nakashima, Y. M., Todorovic, S. M., Pereverzev, A., Hescheler, J., Schneider, T. & Lingle, C. J. (1998). Properties of Ba^{2+} currents arising from human alpha1E and alpha1E-beta3 constructs expressed in HEK293 cells: physiology, pharmacology, and comparison to native T-type Ba^{2+} currents. *Neuropharmacology* **37**, 957–972.

Neelands, T. R., King, A. P. & Macdonald, R. L. (2000). Functional expression of L-, N-, P/Q-, and R-type calcium channels in the human NT2-N cell line. *Journal of Neurophysiology* **84**, 2933–2944.

Newcomb, R., Szoke, B., Palma, A., Wang, G., Chen, X., Hopkins, W., Cong, R., Miller, J., Urge, L., Tarczy-Hornoch, K., Loo, J. A., Dooley, D. J., Nadasdi, L., Tsien, R. W., Lemos, J. & Miljanich, G. (1998). Selective peptide antagonist of the class E calcium channel from the venom of the tarantula *Hysterocrates gigas*. *Biochemistry* **37**, 15353–15362.

Pereverzev, A., Klöckner, U., Grabsch, H., Vajna, R., Olyschläger, S., Viatchenko-Karpinski, S., Schröder, R., Hescheler, J. & Schneider, T. (1998). Structural diversity of the voltage-dependent Ca^{2+} channel alpha1E subunit. *European Journal of Neuroscience* **10**, 916–925.

Perez-Reyes, E. (1999). Three for T: molecular analysis of the low voltage-activated calcium channel family. *Cellular and Molecular Life Sciences* **56**, 660–669.

Piedras-Renteria, E. S., Chen, C. C. & Best, P. M. (1997). Antisense oligonucleotides against rat brain alpha1E DNA and its atrial homologue decrease T-type calcium current in atrial myocytes. *Proceedings of the National Academy of Sciences of the USA* **94**, 14936–14941.

Piedras-Renteria, E. S. & Tsien, R. W. (1998). Antisense oligonucleotides against alpha1E reduce R-type calcium currents in cerebellar granule cells. *Proceedings of the National Academy of Sciences of the USA* **95**, 7760–7765.

Randall, A. & Tsien, R. W. (1995). Pharmacological dissection of multiple types of calcium channel currents in rat cerebellar granule neurons. *Journal of Neuroscience* **15**, 2995–3012.

Randall, A. D. & Tsien, R. W. (1997). Contrasting biophysical and pharmacological properties of T-type and R-type calcium channels. *Neuropharmacology* **36**, 879–893.

Saegusa, H., Kurihara, T., Zong, S., Minowa, O., Kazuno, A., Han, W., Matsuda, Y., Yamanaka, H., Osanai, M., Noda, T. & Tanabe, T. (2000). Altered pain responses in mice lacking alpha 1E subunit of the voltage-dependent Ca^{2+} channel. *Proceedings of the National Academy of Sciences of the USA* **97**, 6132–6137.

Scamps, F., Vigues, S., Restituito, S., Campo, B., Roig, A., Charnet, P. & Valmier, J. (2000). Sarco-endoplasmic ATPase blocker 2,5-di(tert-butyl)-1,4-benzohydroquinone inhibits N-, P-, and Q- but not T-, L-, or R-type calcium currents in central and peripheral neurons. *Molecular Pharmacology* **58**, 18–26.

Schneider, T., Wei, X., Olcese, R., Costantin, J. L., Neely, A., Palade, P., Perez-Reyes, E., Qin, N., Zhou, J., Crawford, G. D. *et al.* (1994). Molecular analysis and functional expression of the human type E neuronal Ca^{2+} channel alpha 1 subunit. *Receptors and Channels* **2**, 255–270.

Schramm, M., Vajna, R., Pereverzev, A., Tottene, A., Klöckner, U., Pietrobon, D., Hescheler, J. & Schneider, T. (1999). Isoforms of alpha1E voltage-gated calcium channels in rat cerebellar granule cells – detection of major calcium channel alpha1 transcripts by reverse transcription-polymerase chain reaction. *Neuroscience* **92**, 565–575.

Schwenk, F., Baron, U. & Rajewsky, K. (1995). A cre-transgenic mouse strain for the ubiquitous deletion of loxP-flanked gene segments including deletion in germ cells. *Nucleic Acids Research* **23**, 5080–5081.

Sigworth, F. J., Affolter, H. & Neher, E. (1995). Design of the EPC-9, a computer-controlled patch-clamp amplifier. 2. Software. *Journal of Neuroscience Methods* **56**, 203–215.

Soong, T. W., Stea, A., Hodson, C. D., Dubel, S. J., Vincent, S. R. & Snutch, T. P. (1993). Structure and functional expression of a member of the low voltage-activated calcium channel family. *Science* **260**, 1133–1136.

Stephens, G. J., Page, K. M., Burley, J. R., Berrow, N. S. & Dolphin, A. C. (1997). Functional expression of rat brain cloned alpha1E calcium channels in COS-7 cells. *Pflügers Archiv* **433**, 523–532.

Taniguchi, M., Sanbo, M., Watanabe, S., Naruse, I., Mishina, M. & Yagi, T. (1998). Efficient production of Cre-mediated site-directed recombinants through the utilization of the puromycin resistance gene, pac: a transient gene-integration marker for ES cells. *Nucleic Acids Research* **26**, 679–680.

Thompson, S. M. & Schwindt, W. (1991). Development of calcium current subtypes in isolated rat hippocampal pyramidal cells. *Journal of Physiology* **439**, 671–689.

Tottene, A., Moretti, A. & Pietrobon, D. (1996). Functional diversity of P-type and R-type calcium channels in rat cerebellar neurons. *Journal of Neuroscience* **16**, 6353–6363.

Tottene, A., Volsen, S. & Pietrobon, D. (2000). Alpha(1E) subunits form the pore of three cerebellar R-type calcium channels with different pharmacological and permeation properties. *Journal of Neuroscience* **20**, 171–178.

Vajna, R., Klöckner, U., Pereverzev, A., Weiergraber, M., Chen, X., Miljanich, G., Klugbauer, N., Hescheler, J., Perez-Reyes, E. & Schneider, T. (2001). Functional coupling between 'R-type' Ca^{2+} channels and insulin secretion in the insulinoma cell line INS-1. *European Journal of Biochemistry* **268**, 1066–1075.

Vajna, R., Schramm, M., Pereverzev, A., Arnhold, S., Grabsch, H., Klöckner, U., Perez-Reyes, E., Hescheler, J. & Schneider, T. (1998). New isoform of the neuronal Ca^{2+} channel alpha1E subunit in islets of Langerhans and kidney – distribution of voltage-gated Ca^{2+} channel alpha1 subunits in cell lines and tissues. *European Journal of Biochemistry* **257**, 274–285.

Williams, M. E., Marubio, L. M., Deal, C. R., Hans, M., Brust, P. F., Philipson, L. H., Miller, R. J., Johnson, E. C., Harpold, M. M. & Ellis, S. B. (1994). Structure and functional characterization of neuronal alpha 1E calcium channel subtypes. *Journal of Biological Chemistry* **269**, 22347–22357.

Wilson, S. M., Toth, P. T., Oh, S. B., Gillard, S. E., Volsen, S., Ren, D., Philipson, L. H., Lee, E. C., Fletcher, C. F., Tessarollo, L., Copeland, N. G., Jenkins, N. A. & Miller, R. J. (2000). The status of voltage-dependent calcium channels in alpha 1E knock-out mice. *Journal of Neuroscience* **20**, 8566–8571.

Zhang, J.-F., Randall, A. D., Ellinor, P. T., Horne, W. A., Sather, W., Tanabe, T., Schwarz, T. L. & Tsien, R. W. (1993). Distinctive pharmacology and kinetics of cloned neuronal calcium channels and their possible counterparts in mammalian CNS neurons. *Neuropharmacology* **32**, 1075–1088.

Acknowledgements

This research was supported by a University of Bonn Medical Center grant 'BONFOR' (H.B.), the German-Israel collaborative research program of the MOS and the BMBF (H.B.), a grant from the Deutsche Forschungsgemeinschaft (DFG EL 122/7) and the Center of Molecular Medicine Cologne/Zentrum für Molekularbiologische Medizin Köln (BMBF 01 KS 9502 to T.S.). We are grateful to Professor Klaus Rajewsky and Drs Werner Müller and Ralph Kühn for their helpful gifts of reagents. We thank Professor M. Taniguchi for the pCre-pac vector. We thank, Dr Xio-hua Chen and Dr George Miljanich for their support, Dr Wolfgang Nastainczyk (Universität des Saarlandes, Homburg) for the synthesis of peptides and antibodies, and Professor Y. Yaari for a critical revision of the manuscript.